DOI: 10.1002/ange.201108345

Drug Design

A Glycosyltransferase Inhibitor from a Molecular Fragment Library Simultaneously Interferes with Metal Ion and Substrate Binding**

*Rene Jørgensen, Lena Lisbeth Grimm, Nora Sindhuwinata, Thomas Peters, and Monica M. Palcic**

Dedicated to Professor Hans Paulsen on the occasion of his 90th birthday

Glycosyltransferases (GTs) are ubiquitous enzymes that form glycosidic bonds by the transfer of monosaccharides from donors, typically nucleotide sugar donors, to carbohydrate, protein, lipid, nucleic acid, or natural product acceptors.[1,2] As each glycosidic linkage requires a different enzyme, the GT class of enzymes is enormous and is encoded by approximately 1% of the genes that have been sequenced to date. GTs are implicated in normal and abnormal biological processes, such as cellular adhesion, cell signaling, carcinogenesis, and cell wall biosynthesis in pathogens.[3–6] GTs have been linked with pathological conditions, therefore, potent and specific GT inhibitors have long been sought as potential therapeutics. However, the synthetic chemistry for inhibitor production is often difficult.[7,8] Inhibitor design is also complicated by the complex reaction mechanisms of GTs, which undergo conformational changes upon substrate binding and throughout the catalytic cycle.[1,2] Unlike other enzyme classes, the potency of most GT inhibitors that are analogues of GT substrates is relatively limited, and the majority of inhibitors have K_i values that are comparable to or greater than the K_M values for the corresponding substrate.[8] As the binding site for the glycosyl donor is shared by multiple different GTs, it is challenging to design specific inhibitors that are based on donor-site ligands.[7–9] The binding site for the donor is very well defined, with a fairly low (μM) dissociation constant, which makes further improvements difficult. The specificity of GTs is most likely a result of the recognition of the acceptor substrate, and the binding pocket for the acceptor is often shallow and easily accessible. The binding affinity for an acceptor is typically less than for a donor and it is, therefore, possible that potent and specific inhibitors can be obtained by linking a donor derivative with an acceptor-site binder as reported for bisubstrate-type inhibitors of sialyltransferases,[10] as well as β-1,4- and α-1,3-galactosyltransferases.[11,12] Recently, 3-phenyl-5-piperazino-1,2,4-thiadiazole (**1**), a heterocycle that contains benzene and piperazine substituents (Scheme 1) and is designated "compound 382", from the Ro5 Maybridge Fragment Library purchased in 2006 which is the predecessor of the Ro3 library, was demonstrated to be an effective inhibitor of human blood group galactosyltransferase B (GTB).[13] Saturation transfer difference (STD)-NMR spectroscopy experiments showed that **1** competes with the H-disaccharide acceptor (K_M = 88 μM) with an IC_{50} value of 790 μM against the acceptor, as determined by surface plasmon resonance (SPR).[13].

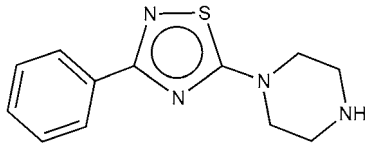

Scheme 1. 3-Phenyl-5-piperazino-1,2,4-thiadiazole (**1**).

Furthermore, docking experiments suggest that the compound occupies part of the acceptor binding site.[13] GTB uses uridine diphosphate galactose (UDP-Gal) as a donor substrate and transfers Gal to α-L-Fuc*p*-(1→2)-β-D-Gal*p* (H-antigen) acceptors, which produces blood group B structures. The closely related enzyme *N*-acetylgalactosaminyltransferase A (GTA) uses UDP-GalNAc as a donor substrate and transfers GalNAc to H-antigen acceptors, which produces blood group A structures. GTA and GTB are highly homologous enzymes that differ by only four amino acid residues (Arg/Gly176, Gly/Ser235, Leu/Met266, and Gly/Ala268). To establish the basis for the selectivity and binding of **1** we have carried out enzyme inhibitor studies by using **1** with GTB, GTA, a GTA/GTB chimeric enzyme and three other related GTs. We have also determined the crystal structure of **1** bound to both GTB and the chimeric enzyme. The chimeric enzyme was weakly inhibited by **1**. To further elucidate the mode of binding by this compound, we tested donor displacement by SPR and STD-NMR spectroscopy. The data show that binding of **1** is specific for GTB. The compound interferes with both acceptor and donor binding and displaces the Mn^{2+} ion in an unprecedented mode of glycosyltransferase inhibition.

Compound **1**, which was previously identified in a library screen as competitive inhibitor of the GTB acceptor binding

[*] Dr. R. Jørgensen, Prof. M. M. Palcic
Carlsberg Laboratory
Gamle Carlsberg Vej 10, 1799 Copenhagen V (Denmark)
E-mail: monica.palcic@carlsberglab.dk
L. L. Grimm, N. Sindhuwinata, Prof. T. Peters
Institut für Chemie, Universität zu Lübeck (Germany)

[**] We thank T. G. Larsen and M. H. Bien for excellent technical assistance during this research. We are grateful for help with X-ray data collection provided by the beamline staff at beamline ID14-4 at the ESRF, Grenoble, France and beamline BL14.1 at BESSY II, Berlin, Germany. This work was supported by the Danish Natural Science Research Council (FNU to M.M.P).

Supporting information for this article is available on the WWW under http://dx.doi.org/10.1002/anie.201108345.

site, was evaluated for its selectivity with a panel of GT enzymes. Standard radiochemical assay formats were adapted for competition studies by co-incubating the enzyme with substrates and various concentrations of **1**. We obtained a K_i value of 800 μM for **1** binding to GTB by using Dixon plots (Table 1). Compound **1** inhibits bovine α-1,3-GalT fivefold more weakly than GTB, with a K_i value of 6.3 mM,

Table 1: Inhibition of wild-type and chimeric blood group A and B enzymes and three other GTs by **1**.

Enzyme	K_i [mM][a]	Acceptor K_M [mM]	Donor K_M [mM]
GTB	0.8	0.088[b]	0.027[b]
AAGlyB	>15.0	0.021[c]	0.0007[c]
GTA	5.1	0.010[b]	0.009[b]
α-1-3-GalT	6.3	0.19	0.077[c]
α-1,4-GalT	n.i.	>0.25	0.0005[c]
β-1,4-GalT	n.i.	0.13	0.022[c]

[a] The K_i values for **1** and various GTs were determined by linear regression analysis of Dixon plots at concentrations of acceptor at the K_M value or lower, UDP-Gal (50 μM), (or UDP-GalNAc for GTA) and **1** (0, 333, 667, 1667, and 3333 μM). [b] Previously reported.[18] [c] Previously reported.[16] n.i. = no inhibition.

but did not inhibit α-1,4-GalT from *Neisseria meningitidis* or bovine β-1,4-GalT (Table 1). Compound **1** has a K_i value of 5 mM for GTA and is a very weak inhibitor of the chimeric enzyme AAGlyB (Arg176, Gly235, Gly266, Ala268), with a K_i value of more than 15 mM. The chimeric enzyme was identified in the murine genome[14] and has dual specificity by utilizing UDP-Gal and UDP-GalNAc donors with equal efficiency to produce both blood group A and B structures. For all of the inhibited enzymes the effect of the inhibitor leveled off at inhibitor concentrations above 3–4 mM, which caused problems with evaluations with GTA and AAGlyB. This is attributed to the low solubility of **1**. Similar findings of reduced inhibition at higher inhibitor concentrations have been reported.[15] The donor K_M value for AAGlyB is 0.7 μM[16] compared to 27 μM for GTB.[17] When the K_i value for **1** binding to AAGlyB was evaluated with 1 μM UDP-Gal, a K_i value of 4.5 mM was obtained, which indicates that **1** also interferes with donor binding.

To better understand the basis for the differential potencies of inhibition of GTB and AAGlyB, we determined the crystal structure of each enzyme in complex with **1**. Both structures were solved by molecular replacement and refined by using X-ray diffraction data sets collected at 1.6 Å resolution for AAGlyB–**1** and 1.85 Å resolution for GTB–**1** (Table S1 in the Supporting Information). The GTB–**1** structure has an overall conformation that is isomorphous with previously described GTB structures (Figure 1 A).[17,19] The internal loop (residues 176–199) is in an "open" conformation with residues 175–181 in chain A and 175–184 in chain B being disordered.

This open and disordered conformation is also seen in the previously solved structures of apo-GTB (PDB entries 2RIT and 1LZ7). A significant difference between the GTB–**1** structure and previously published GTB structures with an "open" conformation is that the C terminus (residues 346–353) of chain A in GTB–**1** is very well ordered and adopts a position that points away from the UDP binding site, which leaves the binding site completely open (see Section 2 in the Supporting Information). The AAGlyB–**1** structure (Figure 1 B) also has an overall conformation that is isomorphous with the previous structures of GTB and AAGlyB.[16] The AAGlyB–**1** complex adopts a "semi-closed" conformation with the internal loop (residues 176–199) isomorphous with the previous AAGlyB–UDP structure.[16] The internal loop is significantly ordered with all of the backbone atoms and most of the residue side chains very well defined. The kink in the α helix (α3) of the internal loop around Arg198, which was described earlier in the "semi-closed" and "closed" GTB structures,[17] is shifted slightly towards Cys196. As usual for the "semi-closed" conformation, the last nine residues at the C terminus (residues 346–354) in the AAGlyB–**1** structure are disordered. The GTB–**1** structure has excellent electron density for the entire inhibitor in the active site of the enzyme (Figure 2 A). There is a strong electron density peak

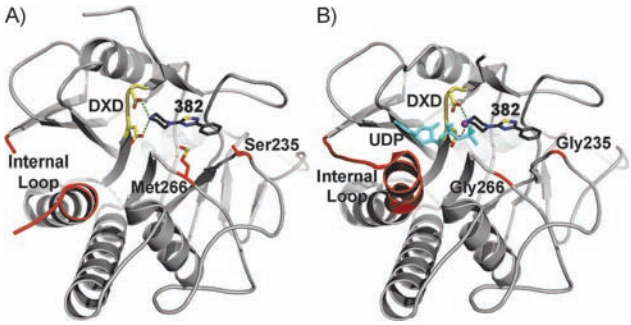

Figure 1. Crystal structures of human blood group GTs. 382 = **1**. A) Structure of GTB–**1**. Hydrogen bonds are indicated by green dotted lines. B) Structure of AAGlyB–**1**. Mn^{2+} ion = purple.

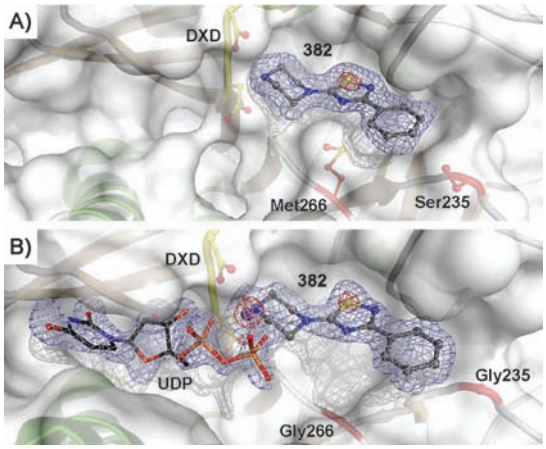

Figure 2. Electron density maps of the enzyme active site. 382 = **1**. A) The substrate binding site for GTB; an F_o-F_c electron density omit map around **1**. Blue density is contoured at 4 σ whereas red density is contoured at 20 σ to emphasize the strong peak of the sulfur atom. B) The substrate binding site for AAGlyB; an F_o-F_c electron density omit map around **1** and UDP. Blue density is contoured at 3.5 σ and red density at 15 σ. In this structure there is also a strong peak at the position of the Mn^{2+} ion. This suggests an inability to completely displace the metal ion and may explain the weaker inhibition of this mutant by **1**.

that corresponds to the sulfur in the five-membered ring of the inhibitor, which confirms the origin of the density as well as the orientation of the compound. The N4 atom of the piperazine ring forms hydrogen bonds to residues Asp211 and Asp213 of the DXD motif, and is placed almost exactly where the metal ion is normally positioned. The remainder of the inhibitor is placed in a predominantly hydrophobic, yet slightly negatively charged pocket, which consists of Met214, Pro234, Ser235, Met266, Ala268, Leu324, Asp 326, Leu329, Leu330, and Ala343 (Figure 3).

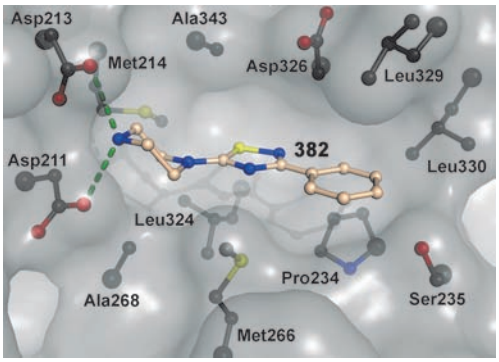

Figure 3. Residues in GTB surrounding the binding pocket for **1**. 382 = **1**.

Thus, the inhibitor directly overlaps with both the fucose moiety of the acceptor and the Mn^{2+} ion (see the structure of AABB–UDP-Gal–acceptor in Figure S3 in the Supporting Information and GTB–**1** in Figure 1 A for comparison), which prevents binding to the active site. The structure of AAGlyB–**1** also has unambiguous electron density for the inhibitor in the same place as in GTB–**1** (Figure 2 B). In AAGlyB–**1**, the outer nitrogen atom of the piperazine ring also forms hydrogen bonds to residue Asp211 and Asp213 (Figure 1 B). As well as a strong peak at the sulfur position in the inhibitor, there is an equally strong peak at the tip of the piperazine ring, which corresponds to the position of the Mn^{2+} ion and indicates that the inhibitor is not able to fully displace the metal ion. Furthermore, there is considerable, yet not fully occupied, density for a UDP molecule in the donor binding site. UDP is used during the final elution step of enzyme purification and trace amounts can remain bound to the donor binding site even after extensive dialysis. With UDP and Mn^{2+} bound in the active site, the position of the piperazine ring of **1** not only occupies the same space as the Mn^{2+} ion, but also clashes severely with the β-phosphate group of the UDP. Therefore, it is highly unlikely that the Mn^{2+} ion can stay bound together with the inhibitor, and UDP will either be displaced or, at least, the β-phosphate group will have to relocate to accommodate **1**. However, there is no indication of an alternative position of the β-phosphate group in the electron density map. By refining the occupancy of the ligands in the binding site with the Phenix refinement program, the occupancy of **1** is refined to 56% in chain A and 63% in chain B. The UDP in chain B, with occupancy of only 37%, has very poor electron density, and the α-phosphate group as well as the ribose ring are the most visible. Correspondingly, in the final refined $2F_o-F_c$ electron density map, the peak for the Mn^{2+} ion in chain B is clearly visible, yet significantly weaker ($\sigma = 6.5$, B-factor 20.9 Å^2) relative to chain A ($\sigma = 7.5$, B-factor 19.5 Å^2). However, the limited presence of the Mn^{2+} ion supports the UDP also being bound at low occupancy.

Biacore experiments were carried out to further probe the displacement of the metal ion by **1**. GTB, AAGlyB, and GTA were immobilized on CM5 chips and dissociation constants were determined from analysis of the binding curves with increasing amounts of **1**. The results clearly support that **1** has a higher binding affinity for GTB than for AAGlyB and GTA (Figure 4; see also Table S2 in the Supporting Information).

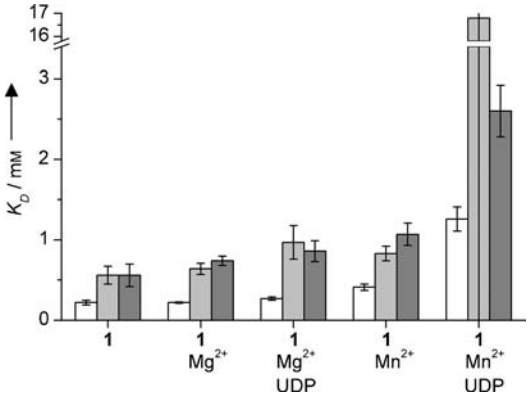

Figure 4. Dissociation constants for GTB (white), AAGlyB (light gray), and GTA (dark gray) with **1** derived from SPR experiments. Measurements were performed on immobilized enzymes in MOPS (50 mM, pH 6.7), NaCl (100 mM), Mg^{2+}/Mn^{2+} (5 mM), UDP (1 mM), **1** (0.25 μM–7 mM). See Table S2 in the Supporting Information for details.

With Mg^{2+} ions present, the dissociation constants were determined to be 0.2 mM for GTB, 0.6 mM for AAGlyB, and 0.7 mM for GTA. However, when comparing a one-site binding model with a two-site binding model, the two-site binding model yields a significantly better fit to the experimental data. This indicates that **1** also adheres to other portions of the protein surface, albeit with much lower binding affinity (Table S2 and Figures S4–S7 in the Supporting Information). The same results were obtained for the other mutants and may be interpreted as unspecific (low affinity) binding that overlays specific binding. Furthermore, the Biacore experiments show that the inhibitory effect of **1** is reduced dramatically when both UDP and Mn^{2+} ions are present. This suggests that UDP–Mn^{2+} complexes bind more tightly to the enzymes than UDP–Mg^{2+} complexes, as the UDP–Mg^{2+} complexes are more easily displaced by **1**.

To derive binding epitopes at atomic resolution, STD-NMR spectra were measured for **1** binding to GTB in the presence or absence of UDP (Figure S8 in the Supporting Information). The piperazine ring of **1** receives less saturation than the phenyl ring. In the presence of UDP, the intensity of the STD signals of **1** is reduced. This suggests that UDP also competes with the binding of **1**.

The SPR and kinetic data show that the binding of **1** is influenced by both the nature of the metal and UDP concentration. Compound **1** has a higher binding affinity for GTB relative to GTA, and at high concentrations of UDP and Mn^{2+} ions there is hardly any detectable binding to the AAGlyB mutant. This enzymological profile is rather unexpected because the crystal structures of both GTB–**1** and AAGlyB–**1** clearly show binding of **1** to the active site of both GTB and the AAGlyB chimera. Binding of **1** is found not only to interfere with the fucose moiety of the disaccharide H-antigen acceptor, but also to displace the Mn^{2+} ion from the position where it is coordinated by the DXD motif and the pyrophosphates of the nucleotide. Furthermore, the structural data suggest that **1** overlaps with the β-phosphate group of the UDP, thereby making the compound a two-substrate inhibitor. This could make **1** a candidate for linking to UDP or uridine monophosphate (UMP) to develop a highly specific and more tightly binding inhibitor. The **1** binding site in the crystal structures of the enzymes differs from that predicted by the Autodock program.[13] Autodock predicts that **1** overlaps with the galactose moiety of the acceptor, whereupon the inhibitor forms a stacking interaction with Trp300, and the N4 atom of the piperazine ring forms a hydrogen bond to Asp302. Interestingly, the two crystal structures also show that the shape of the **1** binding pocket is highly dependent on both residues 235 and 266. In GTB Ser235 and Met266 play a key role in forming a tightly fitting binding pocket for the inhibitor (Figure 2A; see also Figure S9A in the Supporting Information). In AAGlyB, both residues 235 and 266 are glycine residues and although the surface potential does not seem to change significantly, this generates an opening at the bottom of the pocket (Figure 2B; see also Figure S9B in the Supporting Information). Furthermore, the opening of the binding pocket is supported by interface calculations of **1** binding to GTB and AAGlyB, respectively (Table S9 in the Supporting Information), with a greater buried surface area for GTB upon binding to **1**. It is possible that the opening of the binding pocket prevents **1** from binding as tightly to the enzyme. In GTA, which has a leucine residue at position 266 instead of a methionine, the surface potential of the binding pocket also does not significantly change; however, Leu266 maintains a relatively closed and tightly fitting binding pocket (Figure S9C in the Supporting Information). Structures showing that **1** is overlapped with the UDP binding site are supported by SPR experiments, which show that the K_D value of the inhibitor increases dramatically when UDP and Mn^{2+} ions are present. Compound **1** binds weakly to the structurally similar α-1,3-GalT but does not bind to the more distantly related α-1,4- and β-1,4-GalT. The reason that **1** binds to α-1,3-GalT is difficult to explain from a structural perspective. When superimposing the structure of α-1,3-GalT in complex with UDP-Gal and an acceptor analogue (PDB entry 1GX4) onto the structure of GTB, several residues in α-1,3-GalT seem to sterically interfere with the **1** binding site (Figure S10 in the Supporting Information). Therefore, this enzyme does not appear to have a binding pocket that resembles that in human blood group GTs, and it is unlikely that **1** binds to the same site in α-1,3-GalT.

Taken together, these studies show that **1** is a specific ligand for the blood group GTs that competes with the natural acceptor, displaces Mn^{2+} ions, and also sterically interferes with donor binding. Compound **1** binding is very sensitive to the metal ion and to the environment of the binding pocket, especially to the nature of residue 266, and seems to preferentially bind to GTB. Residue 266 is known to be important for the discrimination between Gal and GalNAc transfer, and these **1** binding studies further suggest that replacement of residue 266 can completely change the binding properties of the active site. Therefore, **1** is not only a good candidate for further development of GTB inhibitors, but it is also proving to be a useful molecule in trying to understand the reaction mechanism of GTs.

Experimental Section

All enzymes were cloned and expressed as previously described[20–23] apart from β-1,4-GalT (Sigma–Aldrich). The K_M values for UDP-Gal, UDP-GalNAc, and the α-L-Fuc*p*-(1→2)-β-D-Gal*p*-O-$(CH_2)_7$-CH_3 acceptor with the blood-group enzymes were determined previously[16,18] by a standard radiochemical assay.[17,19] The K_i values for **1** with GTB, GTA, AAGlyB, and α-1,3-GalT were determined by linear regression analysis of Dixon plots by using donor (50 μM) and acceptor (K_M value or lower concentration, see the Supporting Information). The K_i values are based on the average of duplicate experiments and the lowest calculated R^2 value from the fitted lines of each experiment (except for AAGlyB and GTA) was 0.97. For AAGlyB and GTA, there was a significant scattering among the measurements, which resulted in linear fits with very low R^2 values. Therefore, the K_i values for these enzymes were measured up to five times. Crystals were obtained by vapor diffusion against a reservoir solution of PEG-3350 (23%), ammonium sulfate (300 mM), 3-(*N*-morpholino)propanesulfonic acid (MOPS, 50 mM, pH 7), and $MnCl_2$ (50 mM) for GTB, and PEG-3350 (6–9%), ammonium sulfate (50–200 mM), MOPS (50 mM, pH 7), and $MnCl_2$ (50 mM) for AAGlyB. After of a drop (6 μL) of cryo-solution (reservoir solution with no $MnCl_2$, glycerol (30%), and **1** (30 mM, Maybridge) was added to the crystals, the crystals were flash frozen in liquid N_2. X-ray diffraction data on GTB–**1** was collected at the European Synchrotron Radiation Facility (ESRF), Grenoble, France, and data on AAGlyB–**1** was collected at the Berliner Elektronenspeicherring-Gesellschaft für Synchrotronstrahlung (BESSY II). Berlin, Germany. Both data sets were integrated and scaled by using the XDS package.[24] The structures were solved by molecular replacement by using the $CCP4_i$ module Phaser[25] with GTB (PDB entry 2RIT) as a search model. Initial refinement was carried out by using REFMAC5[26] before iteratively rebuilding the structure in Coot,[27] and finally refining in Phenix[28] including translation/libration/screw motion (TLS) determination. Structure quality statistics are given in Table S1 in the Supporting Information. The atomic coordinates and structure factors have been deposited at the Protein Data Bank with the accession codes, 3U0X for AAGlyB-**1** and 3U0Y for GTB-**1**. SPR experiments were performed on a BIAcore 3000 instrument (GE Healthcare) at 298 K. GTB, AAGlyB, and GTA were immobilized on CM5 sensor chips (Biacore) by using the standard Amine Coupling Kit (Biacore). Different concentrations of **1** (0.25 μM–7 mM) were injected with a flow rate of 10 μL min^{-1} for 3 min to reach equilibrium, and then 4 min of waiting time between injections. Two sets of triplicate experiments were performed, and the data was analyzed with Biacore evaluation software and Origin 7.0. The data was fitted to an equation under the assumption of a two-site binding model. The STD-NMR measurements were performed in 3 mm NMR tubes. NMR experiments were carried out on a Bruker Avance DRX 500 spectrometer equipped with a TCI cryogenic probe head. Spectra were recorded at

298 K with the standard STD pulse sequence stddiff.3 and a 10 ms, 7 kHz spin-lock pulse[29] to reduce the background protein resonances. Additional details are in the Supporting Information.

Received: November 27, 2011
Published online: March 8, 2012

Keywords: glycosyltransferases · NMR spectroscopy · surface plasmon resonance · X-ray crystallography

[1] L. L. Lairson, B. Henrissat, G. J. Davies, S. G. Withers, *Annu. Rev. Biochem.* **2008**, *77*, 521 – 555.
[2] J. T. Weadge, M. M. Palcic, *Wiley Encyclopedia of Chemical Biology*, *Vol. 2* (Ed.: T. P. Begley), Wiley, New York, **2008**, pp. 198 – 211.
[3] S. Berg, D. Kaur, M. Jackson, P. J. Brennan, *Glycobiology* **2007**, *17*, 35R – 56.
[4] D. H. Dube, C. R. Bertozzi, *Nat. Rev. Drug Discovery* **2005**, *4*, 477 – 488.
[5] J. D. Marth, P. K. Grewal, *Nat. Rev. Immunol.* **2008**, *8*, 874 – 887.
[6] J. E. Rexach, P. M. Clark, L. C. Hsieh-Wilson, *Nat. Chem. Biol.* **2008**, *4*, 97 – 106.
[7] P. Compain, O. R. Martin, *Bioorg. Med. Chem.* **2001**, *9*, 3077 – 3092.
[8] T. Kajimoto, M. Node, *Synthesis* **2009**, 3179 – 3210.
[9] X. Qian, M. M. Palcic, *Carbohydrates in Chemistry and Biology* (Eds.: B. Ernst, G. Hart, P. Sinaý), Wiley-VCH, Weinheim, **2000**, pp. 293 – 312.
[10] H. Hinou, X. L. Sun, Y. Ito, *J. Org. Chem.* **2003**, *68*, 5602 – 5613.
[11] H. Hashimoto, T. Endo, Y. Kajihara, *J. Org. Chem.* **1997**, *62*, 1914 – 1915.
[12] B. Waldscheck, M. Streiff, W. Notz, W. Kinzy, R. R. Schmidt, *Angew. Chem.* **2001**, *113*, 4120 – 4124; *Angew. Chem. Int. Ed.* **2001**, *40*, 4007 – 4011.
[13] C. Rademacher, J. Landstrom, N. Sindhuwinata, M. M. Palcic, G. Widmalm, T. Peters, *Glycoconjugate J.* **2010**, *27*, 349 – 358.
[14] M. Yamamoto, X. H. Lin, Y. Kominato, Y. Hata, R. Noda, N. Saitou, F. Yamamoto, *J. Biol. Chem.* **2001**, *276*, 13701 – 13708.
[15] Y. Hu, J. S. Helm, L. Chen, C. Ginsberg, B. Gross, B. Kraybill, K. Tiyanont, X. Fang, T. Wu, S. Walker, *Chem. Biol.* **2004**, *11*, 703 – 711.
[16] T. Pesnot, R. Jorgensen, M. M. Palcic, G. K. Wagner, *Nat. Chem. Biol.* **2010**, *6*, 321 – 323.
[17] J. A. Alfaro, R. B. Zheng, M. Persson, J. A. Letts, R. Polakowski, Y. Bai, S. N. Borisova, N. O. Seto, T. L. Lowary, M. M. Palcic, S. V. Evans, *J. Biol. Chem.* **2008**, *283*, 10097 – 10108.
[18] S. L. Marcus, R. Polakowski, N. O. Seto, E. Leinala, S. Borisova, A. Blancher, F. Roubinet, S. V. Evans, M. M. Palcic, *J. Biol. Chem.* **2003**, *278*, 12403 – 12405.
[19] S. I. Patenaude, N. O. Seto, S. N. Borisova, A. Szpacenko, S. L. Marcus, M. M. Palcic, S. V. Evans, *Nat. Struct. Biol.* **2002**, *9*, 685 – 690.
[20] N. O. Seto, M. M. Palcic, C. A. Compston, H. Li, D. R. Bundle, S. A. Narang, *J. Biol. Chem.* **1997**, *272*, 14133 – 14138.
[21] N. O. Seto, M. M. Palcic, O. Hindsgaul, D. R. Bundle, S. A. Narang, *Eur. J. Biochem.* **1995**, *234*, 323 – 328.
[22] J. R. Rich, A. Szpacenko, M. M. Palcic, D. R. Bundle, *Angew. Chem.* **2004**, *116*, 623 – 625; *Angew. Chem. Int. Ed.* **2004**, *43*, 613 – 615.
[23] K. Sujino, T. Uchiyama, O. Hindsgaul, N. O. L. Seto, W. W. Wakarchuk, M. M. Palcic, *J. Am. Chem. Soc.* **2000**, *122*, 1261 – 1269.
[24] W. Kabsch, *J. Appl. Crystallogr.* **1993**, *26*, 795 – 800.
[25] A. J. McCoy, R. W. Grosse-Kunstleve, L. C. Storoni, R. J. Read, *Acta Crystallogr. Sect. D* **2005**, *61*, 458 – 464.
[26] G. N. Murshudov, A. A. Vagin, E. J. Dodson, *Acta Crystallogr. Sect. D* **1997**, *53*, 240 – 255.
[27] P. Emsley, K. Cowtan, *Acta Crystallogr. Sect. D* **2004**, *60*, 2126 – 2132.
[28] P. D. Adams, R. W. Grosse-Kunstleve, L. W. Hung, T. R. Ioerger, A. J. McCoy, N. W. Moriarty, R. J. Read, J. C. Sacchettini, N. K. Sauter, T. C. Terwilliger, *Acta Crystallogr. Sect. D* **2002**, *58*, 1948 – 1954.
[29] M. Mayer, B. Meyer, *Angew. Chem.* **1999**, *111*, 1902 – 1906; *Angew. Chem. Int. Ed.* **1999**, *38*, 1784 – 1788.

